Effects of Atmospheric Gases on the Efficiency of Heating and Cooling Supply Components: Experimental Investigation of Plate Heat Exchangers

Martin Heymann, Franziska Koch and Karin Rühling

Chair of Building Energy Systems and Heat Supply, TU Dresden (GER)

Abstract

The paper presents measurement results for the influence of bubble flow (gas volume fraction up to 6 %) on the pressure drop und heat transfer in three plate heat exchanger test objects, which are operated with water as heat transfer fluid. The gas content effects the efficiency and auxiliary energy consumption of solar thermal systems. Therefore, the plate heat exchanger as one of their main components is investigated in detail.

Keywords: plate heat exchanger, two-phase flow, water, nitrogen, pressure drop, heat transfer

1 Introduction

As is well known, free gases in heat transfer media can cause a wide variety of problems in energy heating systems. In solar thermal systems, for example, these are flow instabilities and partial stagnation. The investigations of the joint research project ImpactGas (Funded by Federal Ministry for Economic Affairs an Climate Action on the basis of a resolution of the German Bundestag, Funding Reference Number: 03EN1001A, research partners Hochschule Zittau/Görlitz and Fraunhofer IFAM Dresden) generally focus on the effects of free gases on the heat output and the pressure loss of individual components. The project team is investigating different types of heat exchangers and is going to study solar thermal collectors. These are the components in solar thermal systems that are expected to have the greatest impact on heat output and hydraulic functioning. The results apply to other types of systems as well.

This paper presents the investigation of three plate heat exchanger test objects. The plate heat exchangers have the same design and differ only in the number of plates. In the following, the component test stand for water/water heat exchangers is presented. It enables the setting of variable gas contents in the heat transfer medium. The measurement concept for determining the flow pressure losses and the heat transfer in the test objects is presented and the influence of free gases with a volume fraction ε of 2 to 6 % is discussed.

The effects of the relevant gases nitrogen, oxygen and carbon dioxide on thermal heating systems are manifold and depend on the control concept used.

In Scenario 1, the control system will try to continue to fulfil the supply task despite a disturbance by free gases. For example, it will increase the heat capacity rate via the pump speed to such an extent, that the target temperature and thus the necessary transmission capacity are reached. For this scenario, it could be shown that the flow pressure losses of all test items increase significantly, but for load cases with at least 50% of the design volume flow only minor effects on the heat transfer are to be expected.

In Scenario 2, the control system cannot compensate for the disturbances caused by the free gases. This can be the case, for example, if the system is already working close to the maximum point or the control only takes into account environmental influences but not process variables. In this case, the total volume flow remains the same, but the heat capacity rate decreases.

doi:10.18086/eurosun.2022.12.07 Available at http://proceedings.ises.org

2 Concept/Methodic

2.1 Heat Exchanger Test Objects

The test objects Hex20, Hex30 and Hex40 are plate heat exchangers from a well-known manufacturer. They have the following parameters:

Tab. 1: Parameters of the plate heat exchanger test objects

Test object	Number of plates	Number of passages	Stamping Angle	Design heat transmission capacity	Design volume flow
			°	kW	m³/h
Hex20	20	1	44 resp. 78	20	0,59
Hex30	30	1	44 resp. 78	30	0,89
Hex40	40	1	44 resp. 78	40	1,19

2.2 Test Rig

Fig. 1 shows the simplified schematic of the component test rig. A well degassed Reference Circuit represents the primary side of the heat exchanger test specimen, i.e. the heating side, and supplies it with temperature-controlled heat transfer fluid.

The so-called Test Circuit supplies the secondary side of the test object with heat transfer medium, which is also temperature-controlled. It has the option to set the gas fraction for dissolved gases (Gas Admission I, not shown here), with nitrogen, technical air and, if necessary, carbon dioxide to produce a defined content of dissolved gases. The heat transfer medium conditioned in this way is stored in a pipe storage tank (not shown here). Gas Admission II can provide a defined fraction of undissolved gases (bubble flow).

All variables required for balancing around the test objects, such as volume flows (F), pressures (P) and the differential pressure (ΔP) as well as the temperatures (T) are measured. The temperatures T21/T22 are the inlet and outlet temperatures on the Test Circuit side, T31/T32 on the Reference Circuit side. For the volume flows, F31 is the sensor on the Reference Circuit side. On the Test Circuit side, there is the sensor F11 located upstream of Gas Admission II which measures the water volume flow $\dot{V}_W$, F12 measures the total volume flow $\dot{V}_W + \dot{V}_G$ accordingly. In the following evaluation, the gas volume flow $\dot{V}_G$ is calculated via the gas mass flow sensor F40, since a higher accuracy can be assumed here. The associated gas volume fraction calculates according to $\varepsilon = \dot{V}_G/(\dot{V}_W + \dot{V}_G)$ – also referred to as void fraction. This definition corresponds to the definition for the homogeneous gas volume fraction according to (VDI-Wärmeatlas, 2013).

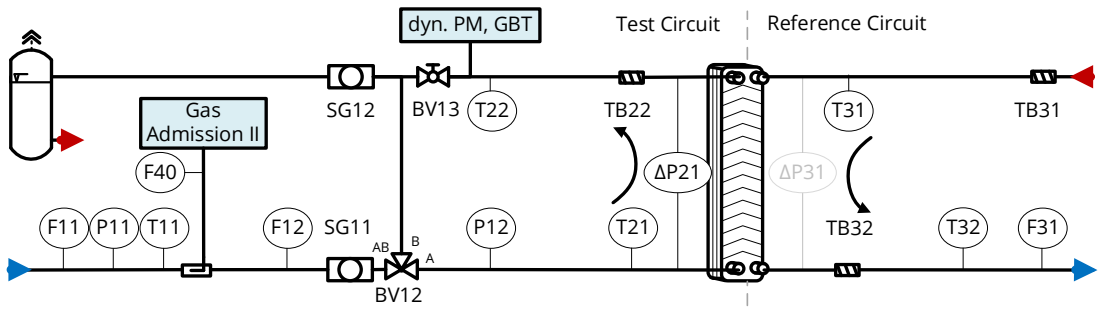

Fig. 1: Component test rig for water-to-water heat exchangers, simplified schematic, F … volume flow sensor, T … temperature sensor, P … pressure sensor dyn. PM ... dynamic pressure maintenance, GBT … "Gas Bubble Test" BV … ball valve, TB … turbulator, SG ... sight glass

The direction of flow was chosen so that the gas-laden side of the heat exchanger test object flows from the bottom to the top. This represents the thermo-hydraulically plausible installation position recommended by the manufacturer. In practice, this should definitely also be taken into account during planning. The side with the greater risk of gas desorption should be flowed through from bottom to top. This is either the circuit with a potential gas entry (e.g. geothermal probe circuit, drinking water, side with compressor pressure maintenance) or the side to be heated, since with water as the heat transfer medium the solubility limit decreases with temperature.

Whether gases have accumulated in the test object during the course of the tests can be determined with a very high degree of accuracy using the measurement method according to (Heymann, et al., 2014) or (VDI 4708-2:2022-04) the so called "Gas Bubble Test". In the heat exchanger component test stand, the inflow of gases via Gas Admission II is first stopped and the test waits until no more gas bubbles can be seen in the SG12 sight glass. Then the pipe section around the test object is shut off by means of the ball valves BV12/BV13 and the pressure is increased via the dynamic pressure maintenance. The initial pressure is restored by draining medium into a collecting vessel. The gas bubble volume can be determined via the measured variables of pressure and volume of drained heat transfer medium. Normalization to the volume of the test circuit side of the test heat exchanger results in the gas volume fraction in the test object $\varepsilon_{\mathrm{Hex}}$.

2.3 Experimental Design

All operating conditions are approached with degassed medium on both sides at first. This represents the Reference Case (RC), which serves as the reference condition for the comparative evaluation. This is followed by the Test Cases (TC) with a well degassed medium (water) at the inlet to the test object and a defined volume fraction of free gases of ε = 2, 4 and 6 %. The selected gas volume fractions correspond to potential conditions in practice. This results in the test matrix shown in Tab. 2. The tests were conceived in such a way that the Reference Case and the Test Case have the same water volume flow $\dot{V}_{\mathrm{W}}$, i.e. they reflect the conditions according to Scenario 1.

The three right-hand columns of Tab. 2 show for which evaluations the tests were used. The column $\varepsilon_{\mathrm{Hex}}$ stands for the investigations on gas accumulation in the test object, Δp and k for the investigations on pressure loss and heat transfer.

Tab. 2: Testing matrix, volume flow rate data in % of the design case

<table>
<tr><td></td><td>Hex20</td><td>Hex30</td><td>Hex40</td><td colspan="4"></td></tr>
<tr><td>Design volume flow</td><td>0,59 m³/h</td><td>0,89 m³/h</td><td>1,19 m³/h</td><td colspan="4"></td></tr>
<tr><td>T31/T21
°C</td><td colspan="3">F31/F11
% of design volume flow</td><td>ε
% (v/v)</td><td>$\varepsilon_{\mathrm{Hex}}$</td><td>$\Delta p$</td><td>$k$</td></tr>
<tr><td>25/25</td><td colspan="3">–/000, –/025, –/050, –/075,
–/100, –/125, –/150, –/175</td><td rowspan="4">RC: 0,
TC: 2,
4,
6</td><td>●</td><td>●</td><td></td></tr>
<tr><td>65/25</td><td rowspan="3">050/050,
-
100/100,
125/125,
150/150</td><td rowspan="3">050/050,
-
100/100,
125/125
-</td><td rowspan="3">050/050,
075/075,
100/100
-
-</td><td></td><td>●</td><td>●</td></tr>
<tr><td>65/35</td><td></td><td>●</td><td>●</td></tr>
<tr><td>75/40</td><td></td><td>●</td><td>●</td></tr>
</table>

The selected test points correspond to the specifications made in DIN EN 1148/A1:2005-12 for the performance testing of water/water heat exchangers. For each heat exchanger, this results in approx. 30 operating conditions in the cold state and in total 36 operating conditions for the tests with heat transfer. After setting the test boundary conditions, a settling time of three minutes is waited for the cold tests and five minutes for the warm tests. These time periods were determined in preliminary tests and are intended to take into account the capacitive effects of heating up the heat exchanger and, if necessary, the accumulation of free gases in the test objects. The measurement time for an operating state set in this way is then two minutes for cold tests and five minutes for warm tests.

The tests at ambient temperature require a significantly shorter test duration, as the conditioning of the Test Circuit and the setting of the test boundary conditions are easier to realize. Therefore, significantly more measuring points were approached for this temperature level (25/25). This means that the influence of the gas loading on the pressure loss in the cold state is particularly well investigated.

A comparable study can be found in the literature (Kreissig & Müller-Steinhagen, 1992). Here, analogous to Scenario 1, the individual tests were compared based on the mass flow density in the flow cross-section. The study investigates the pressure losses of an air-water flow on two plate heat exchangers, for each of which the number of plates can be varied. The aim was to use the air-water flow to model the conditions for the usage as an evaporator. Therefore, the area of investigation with gas volume fractions of up to 100 % differs significantly from the investigation presented here. Furthermore, the flow through the plate heat exchanger was from top to bottom, which complicates the interpretation and evaluation due to the possible accumulation of gases in the test objects.

2.4 Evaluation methodology

In the following, the procedure for evaluating the measurement data will be described in more detail. First, selected calculations are made with the raw measurement data in the time ranges of the steady-state operating conditions. The temporal resolution is one second.

- Further calibration functions are applied to selected measured values in addition to the basic calibration.
- With the pressure and temperature measurement data, the fluid properties (density, specific enthalpy, dynamic viscosity) are determined at the relevant points. These are the inlet and outlet sides of both circuits as well as fluid properties at medium conditions.
- Derived state variables (gas volume fraction), process variables (heat outputs, balance errors) and key Fig.s (pressure loss coefficient, characteristic numbers) are calculated.

For all these variables, averaging takes place over the stationary time range.

- Using the averaged values, selected values (heat transfer coefficient) are calculated.
- An important point of the chosen evaluation methodology is the formation of models for the gas-free Reference Case by means of regressions. These are determined, for example, for the flow pressure losses and the heat transfer, but also for other key Fig.s. In each case, individual trial functions are used that represent the required quantity as a function of the water volume flow and the average temperatures. This procedure makes it possible to assign an exactly matching (modelled) Reference Case to each measured Test Case. In this way, unavoidable variance in the test conditions can be compensated and the validity of the evaluation can be increased.
- The quantities related to the gas-free Reference Case are formed for all Test Cases. The assignment of the Test Case to the Reference Case is carried out for Scenario 1 via the water volume flow rate $\dot{V}_{\mathrm{W}}$. For Scenario 2, the corresponding Reference Case with the same total volume flow $\dot{V}_{\mathrm{tot}} = \dot{V}_{\mathrm{W}} + \dot{V}_{\mathrm{G}}$ can be determined using the model approaches. For the related pressure loss and heat transfer coefficient, the values are calculated according to Equation (1) and (2). For the Reference Case, the model value at volume flow and mean temperature of the Test Case is used:

$$\frac{\Delta p_{\mathrm{f}}}{\Delta p_{\mathrm{f,RC}}} = \frac{\Delta p_{\mathrm{f,TC}}}{\Delta p_{\mathrm{f,RC,Model}}(\dot{V}_{\mathrm{TC}}, T_{\mathrm{m,TC}})} \quad (1)$$

$$\frac{k}{k_{\mathrm{RC}}} = \frac{k_{\mathrm{TC}}}{k_{\mathrm{RC,Model}}(\dot{V}_{\mathrm{TC}}, T_{\mathrm{m,TC}})} \quad (2)$$

The resulting factors can be interpreted analogously to the two-phase multiplier described in (VDI-Wärmeatlas, 2013).

- The determined quantities are plotted against the gas volume flow rate to show the influence of the bubble flow (compare Fig. 3c and 4c). This influence is mapped with a simple (linear) regression function.

According to the (VDI-Wärmeatlas, 2013), the pressure drop of an adiabatic gas-liquid flow in pipelines is composed of

- the acceleration component Δp_{A},
- the hydrostatic component Δp_{g} and
- the actual friction component Δp_{f}.

$$\Delta P21 = p' - p'' = \Delta p_{\mathrm{f}} + \Delta p_{\mathrm{A}} + \Delta p_{\mathrm{g}} \quad (3)$$

The acceleration component Δp_{A} results from a change in momentum of the heat transfer medium if, for example, the flow velocity changes significantly between inlet and outlet, as in an evaporator. This is taken into account in the evaluation, but is negligible for all operating points. With the homogeneous model (see (VDI-Wärmeatlas, 2013) and (Michaelides, et al., 2016)), however, there would be a relevant resulting hydrostatic fraction Δp_{g}, which arithmetically leads to higher friction pressure losses with a measured total pressure. This produces an inconsistent picture in the evaluations and is probably not valid. In the ascending two-phase flow, slip occurs which just compensates the hydrostatic component. Therefore, the evaluation does not consider the hydrostatic component.

In the investigations of (Kreissig & Müller-Steinhagen, 1992) the hydrostatic pressure loss component is considered mathematically. However, in this case, there is a downwards flow and the investigation area is much broader with gas volume fractions of up to 100%. According to the paper, the measurement results were also difficult to reproduce with existing model approaches.

For each operating condition according to Tab. 2, the test boundary conditions are set. These are the inlet temperatures into the test object in the Test and Reference Circuits T21 and T31, the water volume flows in both circuits F11 and F31 as well as the dissolved gas content (here: degassed water) and the gas volume fraction ε set via Gas Admission II. After waiting for the settling time, the outlet temperatures T22 and T32 are set in as the system reaction. The gas bubble volume that may have accumulated $\varepsilon_{\mathrm{Hex}}$ in the test object also represents a system reaction.

3 Results

3.1 Gas accumulation in heat exchanger test objects

For selected tests in the cold state (25/25), the accumulated volume of free gases was determined using the methodology described above ("Gas Bubble Test") and the gas volume fraction in the test specimen $\varepsilon_{\mathrm{Hex}}$ was calculated. Fig. 2 shows the results for all three of the test objects. From a volume flow of 0.5 m³/h upwards, gas contents of less than 2.5 % (v/v) were measured, with a few exceptions, which is close to the expected measurement accuracy. Here, no significant additional effect of an accumulated gas bubble on the heat transfer or the pressure losses is to be expected. The determined effects are then mainly due to the gas bubbles transported along in the flow.

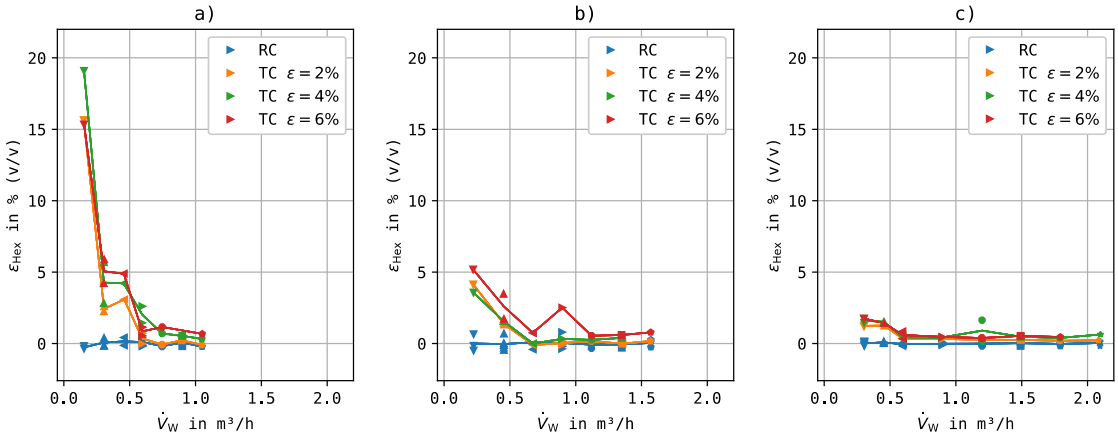

Fig. 2: Gas accumulation, gas volume fraction $\varepsilon_{\mathrm{Hex}}$ in test object, Test Circuit
a) Hex20 with 20 plates, b) Hex30 with 30 plates, c) Hex40 with 40 plates

3.2 Effects on Pressure Drop

Fig. 3 shows measurement results for the pressure loss of test object Hex40 on the Test Circuit side. The tests took place without heating by the Reference Circuit at a media temperature of approx. 25 °C. The gas-free Reference Cases are marked in blue and the Test Cases with a gas volume fraction of ε = 2, 4 and 6 % are shown in yellow, green and red respectively. The gas volume fraction ε is determined with the homogeneous model from the measured values of gas mass flow (F40) and water volume flow (F11) as well as from the corresponding fluid properties. The volume flow F11 corresponds to the volume flow of the pure water $\dot{V}_{\mathrm{W}}$ without the gas component, since the sensor is located upstream of Gas Admission II. It is varied from 0 to approx. 2.1 m³/h (175 % of design volume flow). The evaluation follows the logic of Scenario 1, in which operating states with approximately the same capacity flow rate are compared, which would fulfil very similar supply tasks in practice. An analogue evaluation is available for all three test objects and four temperature levels.

Diagram a) shows the flow pressure loss over the water volume flow rate $\dot{V}_{\mathrm{W}}$. A slight fanning out of the measured values due to an increased gas volume fraction ε can be observed, but general correlations are not yet recognizable in this representation. An empirical model is used to calculate the friction pressure loss Δp_{f} in the Reference Case by means of a trial function depending on volume flow and temperature. The results of the model are shown in the diagram as a blue dotted line.

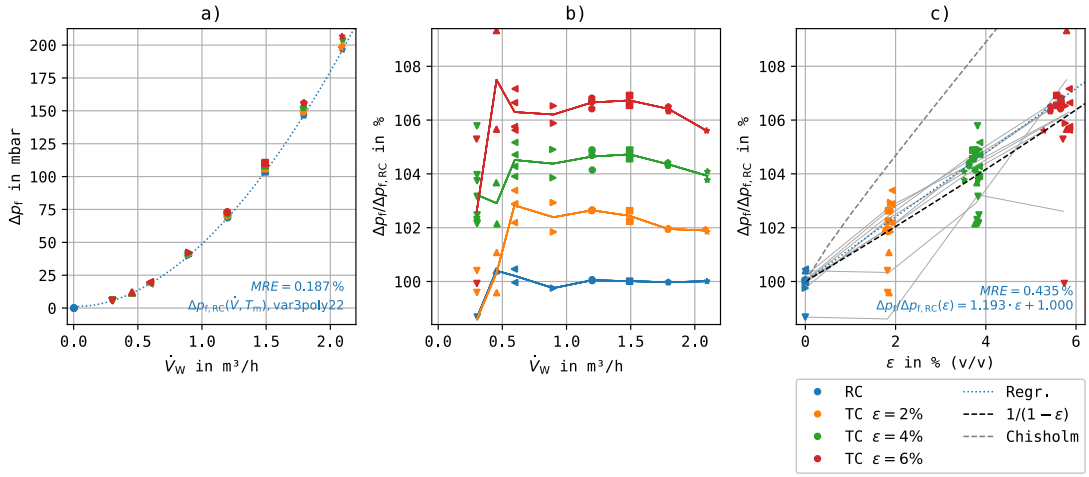

Fig. 3: Flow pressure drop Δp_f in test object Hex40 depending on the gas volume fraction, Scenario 1
a) Plotted over the water flow rate $\dot{V}_W$, reference case model function
b) Related pressure drop $\Delta p_f/\Delta p_{f,RC}$, plotted over the water flow rate $\dot{V}_W$
c) Related pressure drop $\Delta p_f/\Delta p_{f,RC}$, plotted over the gas volume fraction ε, modelling approaches

The modelling of the pressure loss is based on the definition of the pressure loss coefficient ζ in plate heat exchangers from (VDI-Wärmeatlas, 2013) and on a mixed second order polynomial with the volume flow and the mean temperature as variables. The model allows a correction of the Reference Case point in the following.

Diagram b) plots the pressure losses related to the modelled Reference Case $\Delta p_f/\Delta p_{f,RC}$ over the water volume flow $\dot{V}_W$. Significantly increased pressure losses can be seen for the gas-laden Test Cases. In some cases, operating conditions were approached several times. The colored lines in the diagram run along the mean values of these experiments. From a water volume flow $\dot{V}_W$ of 0.5 m³/h, the lines run almost parallel to the abscissa. The related pressure losses here are therefore less dependent on the water volume flow and more on the gas volume fraction ε. Below 0.5 m³/h, the related pressure losses rise sharply in some cases or drop below 100 %. On the one hand, this can be explained by the accumulation of gas cushions (slightly increased values for ε_{Hex}), on the other hand, with the very small numerical values of the measured pressure difference, measurement errors of the sensor and model deviations have a disproportionate effect.

In Diagram c) of Fig. 3 the pressure losses related to the modelled Reference Case $\Delta p_f/\Delta p_{f,RC}$ are plotted over the gas volume fraction ε. The assignment to the volume flow rate is possible via the marking symbol used.

The pressure drop increases steadily with the gas volume fraction ε in the investigated area. The result is a pressure loss that increases by approximately one percentage point per percentage point of gas volume fraction. The measuring points for all volume flows greater than 0.5 m³/h are grouped very closely around a straight line with an increase of 1.2 and with a MRE (Mean Relative Error) of 0.44 %. This is an indication of the high accuracy of the differential pressure sensor used and confirms the evaluation methodology applied. The regression lines $\Delta p_f/\Delta p_{f,RC} = f(\varepsilon)$ were formed for all test objects and temperature pairings and will be discussed later.

The pressure loss coefficient of a two-phase flow ζ is formed according to (Huhn & Wolf, 1975) with effective fluid properties and with a hydraulic diameter defined specifically for plate heat exchangers according to (VDI-Wärmeatlas, 2013). Equation (4) applies to the related pressure loss. With the assumption that the pressure loss coefficients formed in this way depend primarily on the geometry and surface properties of the duct walls (and thus $\zeta/\zeta_{RC} \approx 1$ applies), the following simple approach can be derived:

$$\frac{\Delta p_f}{\Delta p_{f,RC}} = \frac{\zeta}{\zeta_{RC}} \cdot \frac{1}{1-\varepsilon} \approx \frac{1}{1-\varepsilon} \tag{4}$$

This approach is presented in the diagram and follows the measured values of Hex40 very well. The approach described in (VDI-Wärmeatlas, 2013) for predicting the related pressure drop (called Two-Phase Multiplier) according to Chisholm also only assumes a dependence on the gas mass fraction $\dot{x}$ and thus of ε. The related pressure loss $\Delta p_f/\Delta p_{f,RC}$ is thus also seen as independent of the volume flow or the flow velocity. However, this approach leads to a significant overestimation of the gas influence.

3.3 Effect on heat transfer

Fig. 4 shows an example of the measured heat transfer coefficients for test object Hex40 and the temperature level 65/25. An analogous evaluation is available for all three test objects and four temperature levels.

Diagram a) represents the heat transfer coefficients as $k \cdot A$. Here A is the transfer area of the test object taken from the data sheet.

$$k \cdot A = \frac{\dot{Q}_1}{\Delta T_m} \tag{5}$$

The heat transfer coefficient is determined according to Equation (5). Here $\dot{Q}_1$ is the heat flow on the gas-free Reference Circuit side. The heat transfer coefficients increase with increasing water volume flow due to the higher capacity flow, as more heat can be transferred. The determined logarithmic temperature difference ΔT_m also increases. Operating states with higher water volume flow correspond to states with lower Number of Transfer Units NTU (dimensionless heating area). The dimensionless temperature change Φ (operational characteristics) also decreases (not shown here). Diagram a) does not allow any statements about the influence of the gas volume fraction.

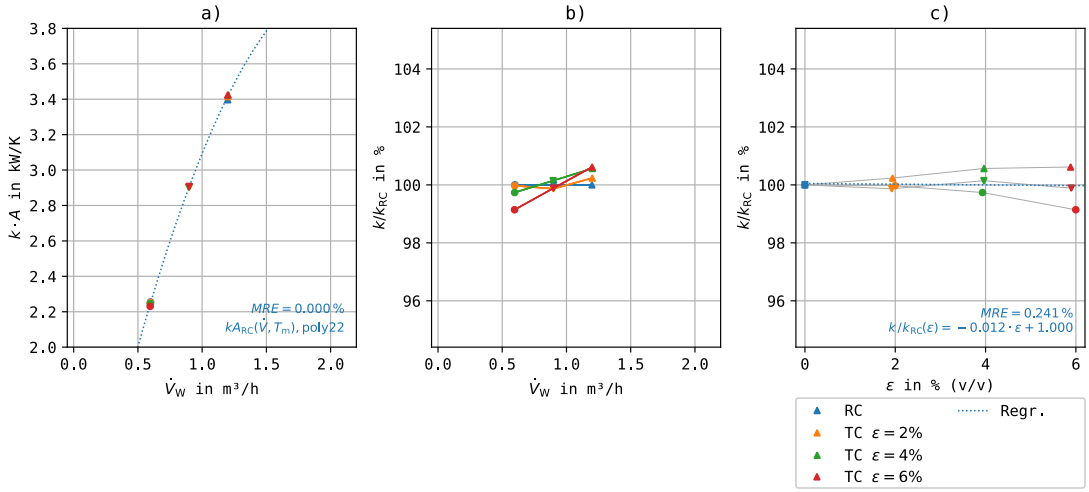

Fig. 4: Heat transfer coefficient k in test object Hex40 depending on the gas volume fraction, Scenario 1
a) Plotted over the water flow rate $\dot{V}_W$, reference case model function
b) Related heat transfer coefficient k/k_{RC}, plotted over the water flow rate $\dot{V}_W$
c) Related heat transfer coefficient k/k_{RC}, plotted over the gas volume fraction ε, modelling approach

Diagrams b) and c) from Fig. 4 show that an increase in the gas volume fraction ε of up to 6 % has only a slight effect on the heat flow coefficients k. The related heat transition coefficient k/k_{RC} varies by a maximum of ±1 %. A slight tendency can be recognized that at high gas volume fractions ε the heat transfer is slightly worse for low volume flow rates and slightly better for high volume flow rates. The deviations are within the range of measurement accuracy and just about balance each other out over all operating points. Regression lines $k/k_{RC} = f(\varepsilon)$ were formed for all test objects and temperature pairs. The gas volume fraction on average shows no influence in the other characteristic Fig.s NTU and Φ in comparison to the Reference Case.

3.4 Overview for all Test Objects and Temperature Levels (Scenario 1 and 2)

In summary, Fig. 5 shows the effects of the bubble flow for Scenario 1. Diagrams a) and b) contain the regressions of the related pressure losses and related heat transfer coefficients for all heat exchanger test objects and investigated temperature pairings. In systems that adjust the water volume flow via a control system so that the supply task is still fulfilled with free gases in the system (Scenario 1), the following statements can be made:

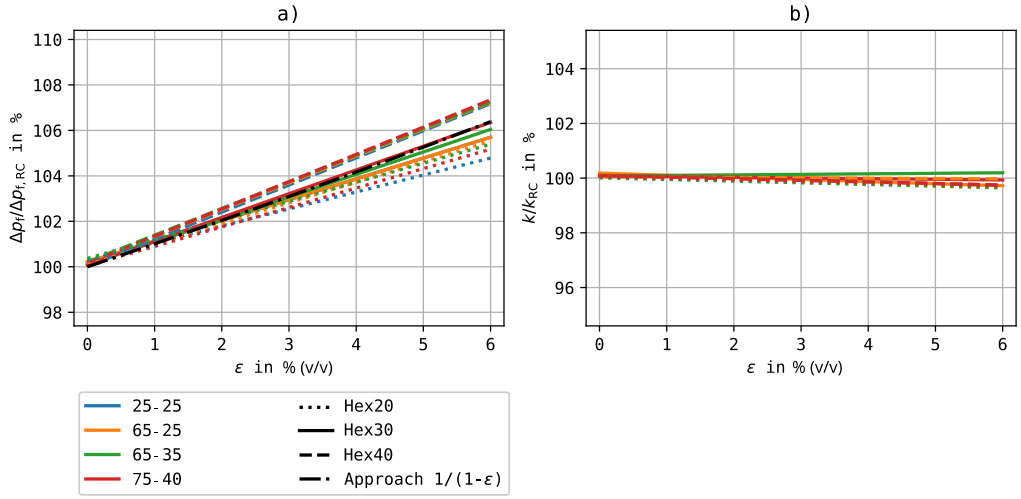

Fig. 5: Overview graph for all heat exchanger test objects and temperature pairings, Scenario 1
a) Related pressure drop $\Delta p_f/\Delta p_{f,RC}$, plotted over the gas volume fraction ε, modelling approach
b) Related heat transfer coefficient k/k_{RC}, plotted over the gas volume fraction ε

The measurements cannot prove an influence of free gases on the heat transfer. Averaged over all volume flows, all regression lines show a gradient close to zero. With a gas volume fraction of 6 %, maximum deviations in the range of ± 0.2 % are to be expected.

Analogously, Fig. 6 shows the evaluation for Scenario 2. In this consideration, the pressure losses according to Diagram a) decrease with increasing gas volume fraction. This results from the fact that the pressure losses of a bubble flow are mainly caused by the viscosity of the water phase and correspondingly lower pressure losses occur at lower water flow velocities. Analogous to the derivation of Equation (4) it can be assumed that the pressure loss coefficients ζ between the Test and Reference Case remain approximately constant for the same water volume flow. With the additional assumption that the deviations in the water volume flow of approx. 6 % according to Scenario 2 only have a minor effect on the ζ-values, the following simple relationship can be derived for Scenario 2:

$$\frac{\Delta p_f}{\Delta p_{f,RC}} \approx 1 - \varepsilon \tag{6}$$

The regressions formed for test objects Hex20 and Hex30 correspond well to this approach for all temperature levels. For Hex40, the pressure losses decrease to a lesser extent. The analysis does not show a relevant influence of the temperature level.

Diagram b) shows a uniform decrease in the heat transfer coefficients k for all test objects and temperature pairings by approx. 4 % at 6 % gas volume fraction. This results from comparing a measured Test Case with a Reference Case with increased water volume flow corresponding to the gas volume fraction. As shown in Fig. 4, the heat flow coefficient increases with increasing water volume flow, which leads to the observed behavior.

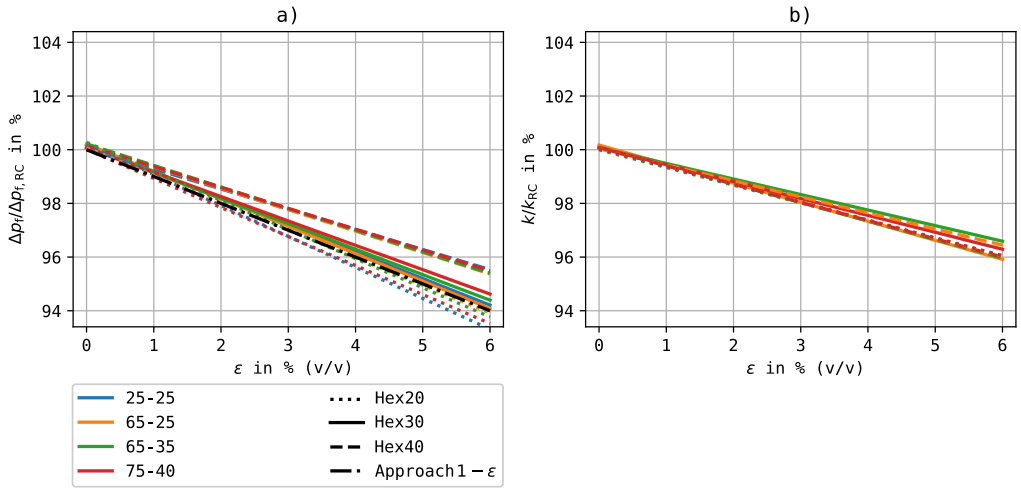

Fig. 6: Overview graph for all heat exchanger test objects and temperature pairings, Scenario 2
a) Related pressure drop $\Delta p_f/\Delta p_{f,RC}$, plotted over the gas volume fraction ε, modelling approach
b) Related heat transfer coefficient k/k_{RC}, plotted over the gas volume fraction ε

4 Conclusion/Prospect

To summarize, the experimental setup can adjust defined two-phase flows of water and free gas components of nitrogen precisely enough. The measurement technology used can represent the effect of variable gas fractions on the pressure loss and heat transfer very well. Circulating free gases in a thermal heating system – e.g. due to lack of care during commissioning or maintenance – can have a negative impact on the system operation.

In systems with a functioning control system, the disturbance caused by air bubbles can be compensated. The supply task can still be fulfilled by increasing the water volume flow via an increasing speed of the circulating pumps until the performance limit is reached (Scenario 1). In this case, however, increased pressure losses (approx. one percentage point per volume percent of gas) in the heat exchanger (and probably other system components) and thus an increased auxiliary energy demand must be expected. The effects on the heat transfer in the heat exchanger are minor in the examined area, possibly slightly depending on the operating condition.

In systems without direct control of the process variables (Scenario 2), the flow pressure losses and the heat transfer decrease accordingly due to the lower water volume flow. However, the supply task can no longer be fulfilled here.

These statements are valid for the selected, favorable mounting orientation of the heat exchanger, in which the flow through the circuit with the greater risk of gas accumulation is from the bottom to the top. It is essential to bear this in mind when designing systems. The strong accumulation of gas cushions in local high points in the system will lead to significant disturbances. At low flow rates, however, gases can accumulate in the heat exchanger even if the installation position is favorable for air removal.

This study highlights a single aspect related to atmospheric gases in the thermal system. Effects on other components such as circulation pumps, fittings, solar thermal collectors, etc. are also to be expected. Temperature and volume flow sensors relevant to control and billing may also be affected.

In any case, increased attention must be paid to the topic during design, commissioning and maintenance. Here, for example, VDI 4708-2 contains important information. It is necessary to always avoid the occurrence of free gases. Care during commissioning and vacuum or membrane degassing can achieve this. For small systems, mobile vacuum degassers that are only used during commissioning and, if necessary, at maintenance dates can be an economical solution. Free gases can be easily detected with a “Gas Bubble Test” and thus the need for action can be evaluated.

Furthermore, the research question is, whether the conclusions gained can be transferred to circuits with water-glycol mixtures.

References/Nomenclature

DIN EN 1148/A1:2005-12. Wärmeaustauscher - Wasser/Wasser-Wärmeaustauscher für Fernheizung - Prüfverfahren zur Feststellung der Leistungsdaten; German version EN 1148:1998/A1:2005. Berlin, Wien, Zürich: Beuth Verlag GmbH, DIN Deutsches Institut für Normung e. V. and DIN-Normenausschuss Kältetechnik (FNKä.). https://dx.doi.org/10.31030/9647845

Heymann, M., Panitz, F., Rühling, K. & Felsmann, C. 2014. Solubility Coefficients for Solar Liquids, a New Method to Quantify Undissolved Gases and Practical Recommendations. Energy Procedia, Band 48, pp. 721-730. https://doi.org/10.1016/j.egypro.2014.02.084

Huhn, J. & Wolf, J. 1975. Zweiphasenströmung gasförmig/flüssig. 1st. Edition. Ed. Leipzig: Fachbuchverlag. https://katalog.slub-dresden.de/id/0-1081515562

Kreissig, G. & Müller-Steinhagen, H. M. 1992. Frictional Pressure Drop for Gas/Liquid Two-Phase Flow in Plate Heat Exchangers. Heat Transfer Engineering, January, Band 13, p. 42–52. https://doi.org/10.1080/01457639208939787

Michaelides, E. E., Crowe, C. T. & Schwarzkopf, J. D. 2016. Multiphase Flow Handbook. CRC Press. https://doi.org/10.1201/9781315371924

VDI-Wärmeatlas. 2013. Verein Deutscher Ingenieure. 11th Edition. Ed. Berlin Heidelberg: Springer. https://doi.org/10.1007/978-3-642-19981-3

VDI 4708-2:2022-04. Druckhaltung, Entlüftung, Entgasung - Entlüftung und Entgasung. Berlin, Wien, Zürich: Beuth Verlag GmbH. https://katalog.slub-dresden.de/id/211-DE88829723

Appendix: Units and Symbols

Tab. 3: Symbols, Abbreviations, Indexes

Quantity	Symbol	Unit
Heat transition coefficient	k	$kW/K/m^2$
Related heat transfer coefficient	k/k_{RC}	%
Number of transfer units	NTU	-
Pressure drop	Δp	mbar
Related friction pressure drop	$\Delta p_f/\Delta p_{f,RC}$	%
Heat flow rate	$\dot{Q}$	kW
Temperature	T	°C
Log mean temperature difference	ΔT_m	K
Volume flow	$\dot{V}$	m³/h
Gas volume fraction or void fraction	ε	% (v/v)
volume fraction of accumulated gas in heat exchanger	ε_{Hex}	% (v/v)
Operational characteristics of heat exchanger	Φ	-
Pressure loss coefficient	ζ	-

Quantity	Symbol
Reference circuit	1
Test circuit	2
Friction	f
Gas	G
Heat exchanger	Hex
Mean relative error	MRE
Reference case	RC
Test Case	TC
Total	tot
Volume fraction	(v/v)
Water	W